Vol. 40 (2009) ACTA PHYSICA POLONICA B No 7

PHYSICS WITH TAGGED FORWARD PROTONS AT RHIC*

Włodek Guryn

Brookhaven National Laboratory, Upton, NY 11973, USA

(Received April 27, 2009)

We describe past, current and future physics program based on triggering (tagging) on forward protons at the Relativistic Heavy Ion Collider (RHIC). This program includes measuring spin dependence in proton–proton elastic scattering, diffractive processes and central production processes. The very forward protons, which remain intact after the scattering of polarized proton–proton collisions at RHIC are detected by detectors placed in the Roman Pots, thus selecting processes, for which the exchange is dominated by one with the quantum numbers of the vacuum, thus enhancing the probability of measuring reactions where colorless gluonic matter dominates the exchange. We present the results obtained by the *pp*2*pp* experiment in polarized proton–proton scattering [S. Bültmann *et al., Phys. Lett.* **B579**, 245 (2004), *Nucl. Instrum. Methods* **A535**, 415 (2004), W. Guryn *et al.*, RHIC Proposal R7 (1994)] and future physics plans, which are based on using Roman Pots of the *pp*2*pp* experiment and the STAR detector K.H. Ackermann *et al., Nucl. Instrum. Methods* **A499**, 624 (2003) at RHIC. The capabilities of the setup to detect Glueballs and Exotics in central production mechanism are described.

PACS numbers: 12.39.Mk, 13.85.Dz, 13.85.Hd, 13.85.Lg

1. Introduction

The Relativistic Heavy Ion Collider (RHIC) with its capability to collide highly polarized proton beams, up to 70% beam polarization, is a unique place to study processes in which scattered protons remain intact after the interaction. At RHIC energies $\sqrt{s}$ =200 GeV and 500 GeV the interaction is dominated by the exchange of a color singlet combination of gluons, two or three gluon exchange. Hence, triggering on forward protons at high (RHIC)

* Presented at the Cracow Epiphany Conference on Hadron Interactions at the Dawn of the LHC, Cracow, Poland, January 5–7, 2009.

energies dominantly selects exchanges mediated by gluonic matter. In addition, the use of polarized proton beams, unique at RHIC, will allow exploring unknown spin dependence of diffraction.

These processes are complementary to the photon diffraction that has already been studied by STAR in Ultra Peripheral Collisions (UPC) of gold–gold (AuAu), and deuteron–gold (dAu) ions, where two pion, $\rho \to \pi^+\pi^-$ [5] and four pion $\pi^+\pi^-\pi^+\pi^-$ photoproduction has been used to probe Pomeron-heavy nucleus couplings.

The protons that remain intact scatter under small angles and their detection is possible using Roman Pots, which are moveable vessels, separating detectors from the vacuum of the accelerator. The movement of the Roman Pots allows placing detectors as close to the beam as background allows in order to measure smallest possible scattering angles, thus extending the t and ξ ranges to the lowest values. Where t is four-momentum transfer squared between the incoming and outgoing protons, $\xi = \Delta p/p$ is the momentum fraction carried off by the Pomeron. This technique is common at the hadron colliders and was first used at the Intersecting Storage Rings (ISR).

We describe results obtained by the *pp*2*pp* experiment in polarized proton –proton elastic scattering in two data runs in 2001 and 2002 [1, 6, 7].

Subsequently the Roman Ports of *pp*2*pp* experiment were moved and installed at STAR detector at RHIC, thus extending physics reach of the original *pp*2*pp* and STAR experiments to include not only elastic processes, but also diffractive processes in which the proton stays intact: Central Production (CP) and Single Diffraction Dissociation (SDD), see Fig. 1. The processes of interest in polarized proton–proton and proton nucleus collisions are [8]: elastic scattering, central production and single diffraction processes. In this paper we shall focus on the first two, Fig. 1. A more detailed description of the physics can be found in [9, 10].

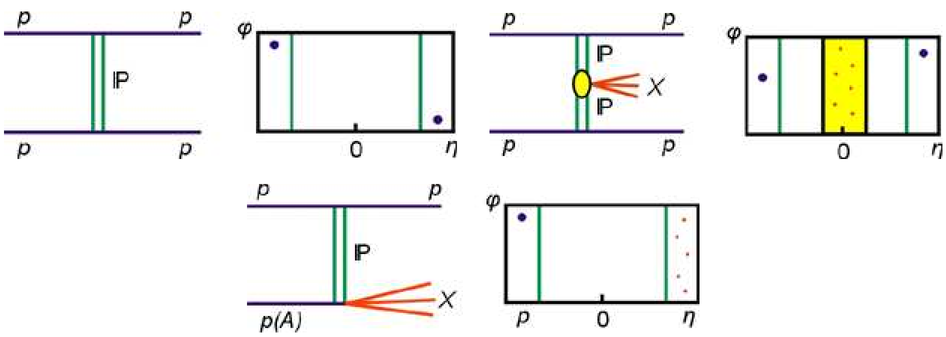

Fig. 1. Diagrams for elastic scattering process (left), central production process (right) single diffraction dissociation (bottom).

2. Elastic scattering

The *pp*2*pp* experiment at RHIC was designed to systematically study polarized proton–proton (*pp*) elastic scattering in $50\,\mathrm{GeV} \leq \sqrt{s} \leq 500\,\mathrm{GeV}$, covering the $|t|$-range from the region of Coulomb Nuclear Interference (CNI) to $1.5\,\mathrm{GeV}^2$.

Studies of spin dependence of *pp* scattering at small momentum transfers and at the highest energies presently available at RHIC offer an opportunity to reveal important information on the nature of exchanged mediators of the interaction, the Pomeron and the hypothetical Odderon, see (Ref. [9, 10] and references therein). The theoretical treatment of small-t scattering is still being developed, hence the experimental data are expected to provide significant constraints for various theoretical approaches and models.

2.1. Results from pp2pp experiment

The first result of the *pp*2*pp* experiment at RHIC on elastic scattering of polarized protons at $\sqrt{s} = 200\,\mathrm{GeV}$ was the measurement of the exponential slope parameter b of the diffractive peak of the elastic cross-section in the t range $0.010 \leq |t| \leq 0.019\ (\mathrm{GeV}/c)^2$ was measured to be $b = 16.3 \pm 1.6$ (stat.) ± 0.9 (syst.) $(\mathrm{GeV}/c)^{-2}$. The slope b for $|t| \leq 0.5\ (\mathrm{GeV}/c)^2$ is inherently sensitive to the exchange process, and its dependence on $\sqrt{s}$ will allow us to

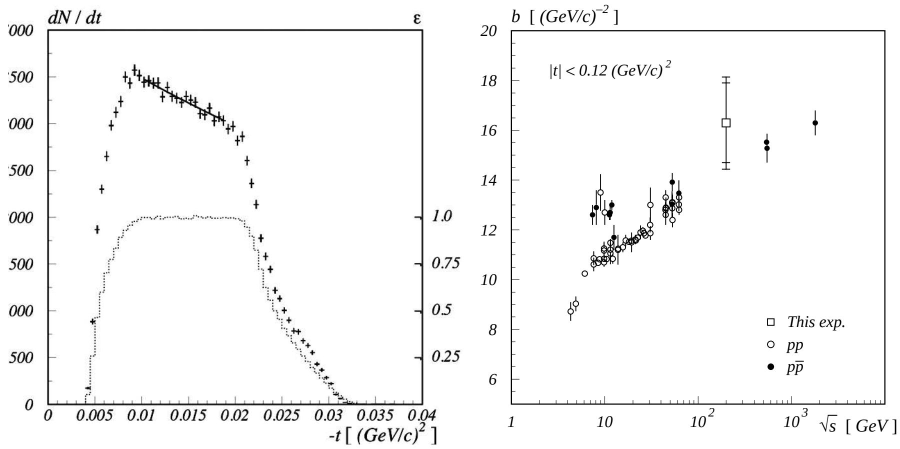

Fig. 2. Left: The distribution of dN/dt within the ϕ region selected as described in the text. The two distributions shown are the measured data and the simulated acceptance function. The fit is shown by the solid line. Right: The result for the slope parameter b of this experiment compared to the world *pp* and $p\overline{p}$ data set. The data are drawn from the Durham Database Group (UK). The error displayed shows both statistical and total errors, where the latter has been computed by a quadrature sum.

distinguish among various QCD based models of hadronic interactions. Some interesting features of b observed in $p\overline{p}$ are not yet confirmed in pp elastic scattering. In general, the forward peak does not show a simple exponential behavior. The t distribution becomes less steep as $|t|$ increases from 0.02 $(\mathrm{GeV}/c)^2$ to 0.20 $(\mathrm{GeV}/c)^2$, although at the highest Tevatron energies this was not observed. It is therefore of interest to see the b behavior in the RHIC energy range, and also to compare the b-values for pp and $p\overline{p}$ elastic scattering. It is expected that they are the same at high energies. However, the $\sqrt{s}$ domain of RHIC is where the difference between pp and $p\overline{p}$ can still be observed.

The next result was the first measurement of the analyzing power A_N in pp elastic scattering of polarized protons at $\sqrt{s} = 200\,\mathrm{GeV}$ and $0.01 \leq |t| \leq 0.03\,(\mathrm{GeV}/c)^2$. A_N is defined as the left–right cross-section asymmetry with respect to the transversely polarized proton beam. In this range of t, A_N originates mainly from the interference between electromagnetic (Coulomb) spin-flip and hadronic (nuclear) nonflip amplitudes [11, 12]. The center of mass energy exceeds by a factor of 10 the energies reached in previous measurements of the elastic scattering spin parameters [16–19].

Polarized pp-elastic scattering is described by five independent helicity amplitudes: two helicity conserving ones ϕ_1 and ϕ_3, two double helicity-flip ones ϕ_2 and ϕ_4, and one single helicity-flip amplitude ϕ_5 (see Ref. [11] for definitions). Each amplitude consists of hadronic and electromagnetic parts; $\phi_i = \phi_i^{\mathrm{em}} + \phi_i^{\mathrm{had}}$.

The A_N in the Coulomb-nuclear interference (CNI) region is a sensitive probe of the hadronic spin-flip amplitude [13]. A possible hadronic single spin-flip amplitude would alter A_N and its effect would depend on the ratio of the single spin-flip amplitude (ϕ_5) to nonflip amplitudes (ϕ_1 and ϕ_3), $r_5 = m\phi_5/(\sqrt{-t}\,(\phi_1 + \phi_3)/2)$, where m is the nucleon mass.

The values of A_N measured by the *pp2pp* experiment and their statistical errors are shown in Fig. 3 for the three t-intervals. The curves shown in the figure represent theoretical calculations using the formula for A_N in the CNI region.

The solid curve in Fig. 3 corresponds to the calculation without hadronic spin flip (Re r_5 and Im r_5 set to 0). To quantify a possible contribution of the single helicity-flip amplitude ϕ_5, the formula was fitted to the measured A_N values with $\mathrm{Re}\,r_5$ and $\mathrm{Im}\,r_5$ as fit parameters. The statistical and systematical errors (except the normalization error) of A_N were added in quadrature for the fit. The results of the fit are following: $\mathrm{Re}\,r_5 = -0.042 \pm 0.037$ and $\mathrm{Im}\,r_5 = -0.51 \pm 0.60$. The dashed line in Fig. 3 represents the curve resulting from the fit.

The fitted values of $\mathrm{Re}\, r_5$ and $\mathrm{Im}\, r_5$ are shown in Fig. 3 together with contours for 1σ, 2σ and 3σ confidence levels. In addition, the point corresponding to no hadronic spin-flip is also shown. The fitted r_5 is hardly compatible, at 2σ level, with the hypothesis of no hadronic spin-flip. However, when the large uncertainty of the beam polarization is taken into account, the present measurement does not allow to exclude the later hypothesis.

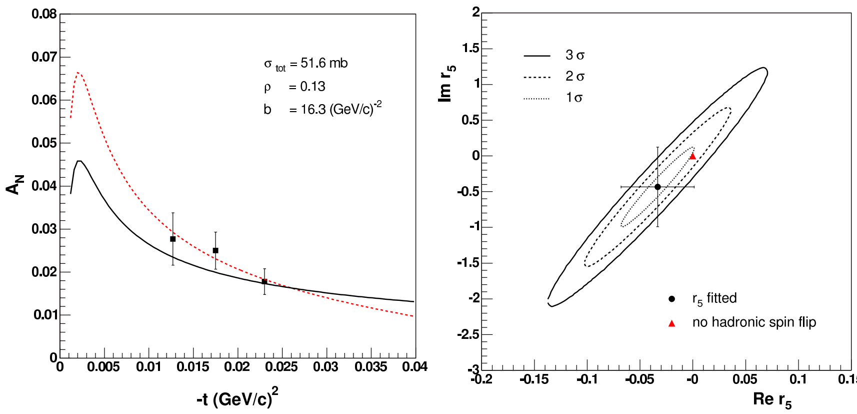

Fig. 3. Left: The single spin analyzing power A_N for three t intervals. Vertical error bars show statistical errors. The solid curve corresponds to theoretical calculations without hadronic spin-flip and the dashed one represents the r_5 fit. Right: Fitted values of r_5 (full circle) with contours corresponding to the different confidence levels. The point corresponding to no hadronic spin-flip (triangle) is also shown.

Recent measurements of A_N at substantially lower cms energies than the one reported here indicate small but significantly different from zero contribution of spin-flip amplitude in case of proton–carbon scattering [16–18] and are consistent with no spin-flip contribution for proton–proton scattering [19] at $\sqrt{s} = 13.7\,\mathrm{GeV}$.

The *pp*2*pp* experiment also measured double spin asymmetries A_{NN} and A_{SS} in elastic scattering of polarized protons at RHIC at $\sqrt{s} = 200$ GeV and low t-range $0.01 \leq |t| \leq 0.03\,\mathrm{GeV}$ [7].

The double spin asymmetry A_{NN} is defined as the cross-section asymmetry,

$$A_{NN} = \frac{\sigma^{\uparrow\uparrow+\downarrow\downarrow} - \sigma^{\uparrow\downarrow+\downarrow\uparrow}}{\sigma^{\uparrow\uparrow+\downarrow\downarrow} + \sigma^{\uparrow\downarrow+\downarrow\uparrow}}\,, \tag{1}$$

for both beams fully polarized along the unit vector $\hat{n}$ normal to the scattering plane. The asymmetry A_{SS} is defined analogously, but for both beams fully polarized along the unit vector $\hat{s}$ in the scattering plane and normal to the beam.

In the small t region the parameters A_{NN} and A_{SS} are sensitive to the interference between hadronic spin-flip amplitudes $\phi_2^{\rm had}$ and $\phi_4^{\rm had}$, and the electromagnetic non-flip amplitude. This provides a sensitive tool to study the spin dependence of diffractive scattering at asymptotic energies and to search of the hypothetical Odderon exchange [20]. Because Pomeron and Odderon have opposite C-parities, it is expected in leading order, that if Pomeron and Odderon have the same asymptotic behaviour, up to logarithms, they are out of phase by approximately 90° [21]. Therefore, if they couple to spin, their interference with the electromagnetic non-flip amplitude will result in different t dependences of the double spin asymmetries.

The results on the double spin asymmetries for the whole t-interval $0.010 \leq -t \leq 0.030$ (GeV$/c)^2$, at an average $\langle -t \rangle = 0.0185$ (GeV$/c)^2$, are presented in Table I. The most accurately determined asymmetry is $A_{SS} = 0.0035 \pm 0.0081$, which is consistent with zero at 1σ confidence level. The asymmetry $A_{NN} = 0.0298 \pm 0.0166$ as well as the combinations $(A_{NN} + A_{SS})/2 = 0.0167 \pm 0.0091$ and $(A_{NN} - A_{SS})/2 = 0.0131 \pm 0.0096$ are also small and consistent with zero.

TABLE I

Double spin asymmetries A_{NN}, A_{SS} for the t-interval $0.010 \leq -t \leq 0.030$ (GeV$/c)^2$ at $\langle -t \rangle = 0.0185$ (GeV$/c)^2$.

	A_{NN}	A_{SS}
Asym	0.0298	0.0035
Δ Asym (stat.+norm.)	± 0.0166	± 0.008
Δ Asym (syst.)	± 0.0045	± 0.003
Δ Asym due to polar. error	± 32.3 %	

Those results, including A_N measurements at lower energies, provide the much needed input for the theoretical calculations of the exchange process. They also underline a need for further measurements to be able to reconcile the differences for a more complete picture to emerge and also to extend the measurements to higher energies. In addition, an extension of the t-range will allow to constrain both the magnitude and the shape of the analyzing power as a function of t, and higher statistics will permit more precise measurements of A_{NN} and A_{SS}. This will be done with the current setup of *pp*2*pp* Roman Pots and the STAR experiment.

2.2. Elastic scattering program with the STAR detector

As mentioned earlier almost the entire energy range, $50\,\mathrm{GeV} \leq \sqrt{s} \leq 500\,\mathrm{GeV}$, of this experiment has been inaccessible to proton–proton scattering, and the measurements above RHIC energies will be made at the Large Hadron Collider [22].

The program described here will improve precision of the measurements already made by the *pp*2*pp* experiment and complete the program of elastic scattering measurements as outlined in the original *pp*2*pp* proposal.The measurement of the differential pp cross-section $d\sigma/dt$ over the extended t-range will include the region at the lower $|t|$ that is particularly sensitive to the ratio of the real to imaginary part of the scattering amplitude the ρ-parameter. This will allow extracting the ρ-parameter and the nuclear slope parameter b in a combined fit to the differential cross-section possible and might also lead to an extraction of σ_{tot}.

An asymptotic difference between the differential and total cross-sections for pp and $p\bar{p}$ could be explained by a contribution of the Odderon to the scattering amplitude. The absence of an Odderon contribution would lead to identical cross-sections, approaching each other roughly as $s^{1/2}$, where s is the center of mass energy squared.

By measuring spin related asymmetries one will be able to determine elastic scattering at the amplitude level [11, 12, 14, 15]. The availability of longitudinal polarization at STAR in this first phase would allow measuring double spin analyzing power for longitudinal spin A_{LL} in addition to double spin analyzing power with transverse A_{NN}, and radial spin A_{SS}, and single spin analyzing power with transverse spin A_N, resulting in a significant improvement of our physics capabilities. Full azimuthal coverage for elastic events has been implemented in this phase.

One of the physics motivations to measure the A_N is to study of the $\sqrt{s}$ dependence of the spin-flip to spin-nonflip amplitudes ratio [15]. In other words it is possible that a small contribution from hadronic spin-flip to the spin single-spin asymmetry, not excluded by measurements at RHIC with a polarized jet target at $p_{\mathrm{lab}} = 100\,\mathrm{GeV}/c$ [19], could increase at $\sqrt{s} = 200\,\mathrm{GeV}$. This will help to reveal long standing problem of the energy dependence of the spin-flip amplitude, which is best answered experimentally.

Using the existing power supplies one can run with optics of $\beta^* = 20\mathrm{m}$ and at $\sqrt{s} = 200\,\mathrm{GeV}$. This optics could extend the t coverage, with 100% acceptance for $0.003 < |t| < 0.03\,(\mathrm{GeV}/c)^2$. Reaching such a small $|t|$-value allows measuring the single spin analyzing power A_N close to its maximum at $|t| \approx 0.0024(\mathrm{GeV}/c)^2$, where $A_{\mathrm{max}} = 0.04(\mathrm{GeV}/c)^2$, at $\sqrt{s} = 200\mathrm{GeV}$. The A_N and its t-dependence in the covered range is sensitive to a possible contribution of the single spin-flip amplitude, ϕ_5 [15], from the interference between the hadronic spin-flip amplitude with the electromagnetic non-flip amplitude. An additional contribution of the hypothetical Odderon to the pp scattering amplitude can be probed by measuring the double spin-flip asymmetry, A_{NN} [15].

Given polarization 50% and 2.3 mb cross-section within our acceptance we shall get 40×10^6 events. In the four t subintervals we shall have $\approx 5 \times 10^6$ events in each. The corresponding errors are $\Delta A_N = 0.0017, \Delta A_{NN} = \Delta A_{SS} = 0.003$.

For the amount of data we expect to collect in 2009, an estimated error on the slope parameter is $\Delta b = 0.31\,(\mathrm{GeV}/c)^{-2}$ and on the ratio of real to imaginary part $\Delta\rho = 0.01$, which is comparable to the existing measurements from the pp and $p\bar{p}$ data.

3. Particle production in the central production process

We describe a scenario of executing the physics program in two phases, which optimizes the use of available resources and maximizes physics output. Phase I has been implemented and is ready to take data in 2009. In the future the physics reach will be extended to higher values of t and larger data samples will be taken. This would be achieved in Phase II, for which a design work is ongoing.

Central Production using Roman Pots and rapidity gap techniques has been studied at all the hadron colliders: ISR [23], S$p\bar{p}$S [24] and the Tevatron [25] and is planned to be studied at the LHC [27] with the aim of discovering low mass Higgs boson. In the Double Pomeron Exchange (DPE) process, see Fig. 1, each proton "emits" a Pomeron and the two Pomerons interact producing a massive recoil system M_X. The massive system M_X could form resonances or jet pairs. Because of the constraints provided by the double Pomeron interaction, glueballs, and other states coupling preferentially to gluons, could be enhanced and produced with much reduced backgrounds compared to standard hadronic production processes. It is also of general interest in QCD to study particle production in the DPE process [26].

In the kinematical region, which we are proposing to cover, those processes allow exploration of the non-perturbative regime of QCD, relying on the strength of the STAR detector: excellent charged particle identification in the central rapidity region and p_{T} resolution, coupled with ability to tag diffractive events with the forward protons with Roman Pots.

Tagging and measuring forward protons also removes the ambiguity of a (complementary) rapidity gap tag, which has a background due to the low multiplicity of diffractive events, and allows the full characterization of the event in terms of t, ξ and the mass of the recoil system M_X.

The idea that the production of glueballs is enhanced in the central region in the process $pp \to pM_Xp$ was first proposed by [28] and was demonstrated experimentally [29]. The crucial argument here is that the pattern of resonances produced in central region, where both forward protons are tagged, depends on the vector difference of the transverse momentum of the final state protons $\vec{k}_{T1}$ and $\vec{k}_{T2}$, with $dP_{\rm T} = |\vec{k}_{T1} - \vec{k}_{T2}|$. The so-called $dP_{\rm T}$ filter argument is that when $dP_{\rm T}$ is large ($\Lambda_{\rm QCD}$) $q\bar{q}$ states are prominent and when $dP_{\rm T}$ is small the surviving resonances include glueball candidates [28, 29].

In what we are proposing, large data samples of diffractive states can be obtained and analyzed as function of diffractive mass M_X and t ($d^2\sigma/dM_X^2dt$) for central production.

We studied the geometrical acceptance of our setup for both SDD and DPE processes. We have generated protons with t and ξ uniformly distributed in the regions $0.003 \leq |t| \leq 0.04(\text{GeV}/c)^2$ and $\xi \leq 0.05$, respectively. We assumed that the Roman Pots are 10mm from the beam center, which is at least 12σ of the beam size at the detection point.

Our studies indicate that there is good acceptance to measure inelastic diffraction processes DPE with $\beta^* = 20\,\text{m}$ optics for Phase I. With the expected luminosity we can collect $\approx 10^5$, accepted DPE events. Number of events for which the proton momentum is reconstructed, where it is required that two RPs on each side are used allowing reconstruction of the outgoing proton momentum, is about factor of four lower. One assumes a 140 μbarn cross-section for the DPE process [30].

Also, as noted earlier, the events seen in the STAR Time Projection Chamber (TPC) in *pp* Central Production are very similar to those in heavy-ion UPC collisions. The tracks in STAR TPC are reconstructed in the full azimuthal angle and in the rapidity interval $|y| \leq 1$. The particle identification is done by measuring specific energy loss dE/dx in the transverse momentum range $p_{\rm t} \leq 1$ GeV/c [31]. The algorithms and reconstruction code that has been developed to deal with those events can also be used in our program. In particular experience gained in dealing with the backgrounds is very valuable.

4. Implementation plan

We will execute the above physics program in two phases. In both phases Roman Pots and STAR detector shall be used, Fig. 4.

In Phase I the existing *pp2pp* experimental set-up, already installed at STAR, will measure spin dependence of both elastic scattering in an unexplored $0.003(\text{GeV}/c)^2 \leq -t \leq 0.03\ (\text{GeV}/c)^2$ and $\xi \leq 0.05$ range, with respect to what has been done already, and of Central Production described above, for which our studies found that there is good acceptance.

In Phase II the Roman Pot system will be installed between DX–D0 magnets, allowing to maximize the acceptance and the range in t, ξ and M_X. In this phase a new system of Roman Pots will be used in conjunction with the STAR TPC to reconstruct and fully constrain events with resonance

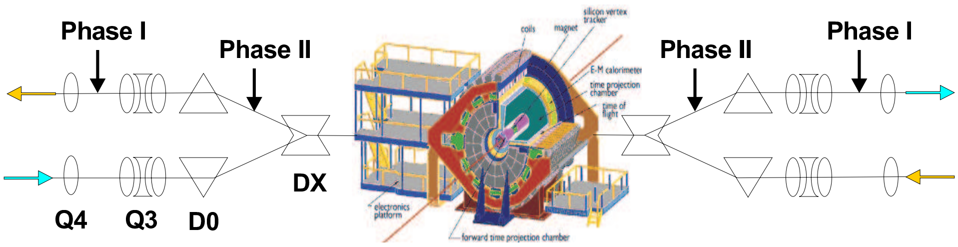

Fig. 4. The Roman Pots of the *pp*2*pp* experiment in the STAR interaction region, with the arrows indicating proposed locations for Phase I and Phase II.

in central production process. The search for exotics is one of the topics of interest here, but not the only one. Since no special accelerator optics is required in this configuration, hence the running in parallel with STAR is possible, we will be able to acquire large data samples of the order 2×10^8 centrally produced triggered events, which is needed in exotic searches.

5. Summary

In summary the physics program with tagged forward protons at STAR will: (1) Study elastic scattering and its spin dependence in unexplored t, ξ and $\sqrt{s}$ range; (2) Study the structure of color singlet exchange in the non-perturbative regime of QCD; (3) Search for diffractive production of light and massive systems in double Pomeron exchange process; (4) Search for new physics, including glueballs and Odderon.

Finally, we stress that the studies we are proposing will add to our understanding of QCD in the non-perturbative regime where calculations are not easy and one has to be guided by measurements.

The research reported here has been performed in part under the US DOE contract DE-AC02-98CH10886.

REFERENCES

[1] S. Bültmann *et al.*, *Phys. Lett.* **B579**, 245 (2004).

[2] S. Bültmann *et al.*, *Nucl. Instrum. Methods* **A535**, 415 (2004).

[3] W. Guryn *et al.*, RHIC Proposal R7 (1994), unpublished.

[4] K.H. Ackermann *et al.*, *Nucl. Instrum. Methods* **A499**, 624 (2003).

[5] C. Adler *et al.*, *Phys. Rev. Lett.* **89**, 272302 (2002); B.I. Abelev *et al.*, *Phys. Rev.* **C89**, 34910 (2008).

[6] S. Bültmann *et al.*, *Phys. Lett.* **B632**, 167 (2006).

[7] S. Bültmann *et al., Phys. Lett.* **B647**, 98 (2007).

[8] A. Bravar, W. Guryn, S.R. Klein, D. Milstead, B. Surrow, *J. Phys. G* **28**, 2885 (2002).

[9] V. Barone, E. Predazzi, High-Energy Particle Diffraction, Texts and Monographs in *Physics* Springer-Verlag, 2002, ISBN: 3540421076.

[10] S. Donnachie, G. Dosch, P. Landshoff, *Pomeron Physics and QCD*, Cambridge University Press, 1998, ISBN: B0006Z3XLM.

[11] N.H. Buttimore, B.Z. Kopeliovich, E. Leader, J. Soffer, T.L. Trueman, *Phys. Rev.* **D59**, 114010 (1999).

[12] N.H. Buttimore, E. Leader, T.L. Trueman, *Phys. Rev.* **D64**, 094021 (2001).

[13] B.Z. Kopeliovich, B.G. Zakharov, *Phys. Lett.* **B266**, 156 (1989); T.L. Trueman, `hep-ph/9610439`.

[14] B.Z. Kopeliovich, *Phys. Rev.* **C68**, 044906 (2003).

[15] T.L. Trueman, `arXiv:0711.4593 [hep-ph]`.

[16] N. Akchurin *et al., Phys. Rev.* **D48**, 3026 (1993).

[17] O. Jinnouchi *et al.*, Proceedings of the 16th International Spin Physics Symposium, SPIN 2004, Eds. F. Bradamante *et al.*, World Scientific, 2005, p. 515.

[18] J. Tojo *et al., Phys. Rev. Lett.* **89**, 052302 (2002).

[19] H. Okada *et al., Phys. Lett.* **B638**, 450 (2006).

[20] E. Leader, T.L. Trueman, *Phys. Rev.* **D61**, 077504 (2000).

[21] R.J. Eden, *Rev. Mod. Phys.* **D43**, 15 (1971).

[22] G. Anelli *et al.* [TOTEM Collaboration], The TOTEM Experiment at the CERN Large Hadron Collider, 2008 JINST 3 S08007.

[23] T. Åkesson, M.G. Albrow *et al., Nucl. Phys.* **B264**, 154 (1986).

[24] A. Brandt *et al.* [UA8 Collaboration], *Eur. Phys. J.* **C25**, 361 (2002).

[25] T. Aaltonen *et al.* [CDF Collaboration], `arXiv:0712.0604v2`.

[26] A. Szczurek, *Acta Phys. Pol. B* **40**, 1877 (2009), these proceedings.

[27] M. Albrow *et al.*, CERN-LHCC-2006-039.

[28] F. Close, *Rep. Prog. Phys.* **51**, 833 (1988); F. Close, A. Kirk, G. Schuler, *Phys. Lett.* **B477**, 13 (2000).

[29] D. Barberis *et al.* [WA102 Collaboration], *Phys. Lett.* **B479**, 59 (2000).

[30] K.H. Streng, *Phys. Lett.* **B171**, 313 (1986).

[31] B. Grube [STAR Collaboration], `arXiv:0808.3991[nucl-ex]`.